

INFLUENCE OF GRAPHENE OXIDES PRODUCED BY DIFFERENT PROCESSING TECHNIQUES ON THE CORROSION RESISTANCE OF ELECTRODEPOSITED Zn-GRAPHENE COMPOSITE COATINGS

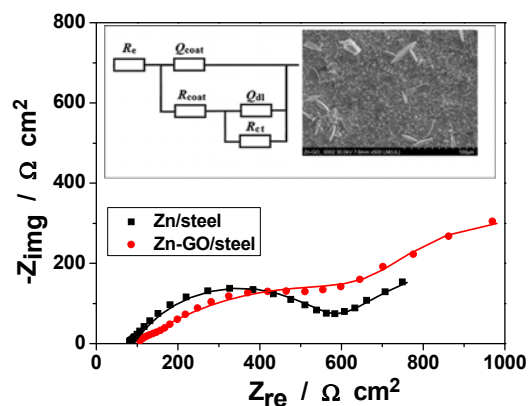
Nicoleta COTOLAN,^a Liviu Cosmin COTET,^a Daniel MARCONI^b and Liana Maria MURESAN^{a,*}

^a Department of Chemical Engineering, Faculty of Chemistry and Chemical Engineering, “Babes-Bolyai” University, 11 Arany Janos Street, 400028 Cluj-Napoca, Roumania

^b Department of Molecular and Biomolecular Physics, National Institute for Research and Development of Isotopic and Molecular Technologies, 67-103 Donath Street, 400293 Cluj-Napoca, Roumania

Received February 5, 2018

The present work is focused on the characterization of new composite zinc electrodeposits containing several graphene oxides produced by different processing techniques, aiming to improve the corrosion resistance of steel substrates. The corrosion behavior of the zinc-graphene composite deposits obtained from an acidic electrolyte (pH = 5.6) at two current densities (20 mA/cm² and 40 mA/cm²) in the presence of several types of graphene oxides produced by graphite exfoliation was investigated. Electrochemical impedance spectroscopy (EIS) and potentiodynamic polarization methods were used to characterize the corrosion behavior of the deposits. The obtained results for Zn/steel, and Zn-graphene/steel deposits were compared in the same experimental conditions. The incorporation of graphene oxide in zinc matrices enhanced the corrosion resistance of the resulting composite coatings when compared to pure zinc coating and the degree of enhancement depends on the graphene oxide nature and preparation mode.



INTRODUCTION

Zinc is widely used as sacrificial coating on mild steel, however its lifespan is limited in aggressive environments.¹ Zn-based protective coatings are preferred over Ni-based coatings as the formation of nano/micro defects in Ni plating can lead to the corrosion of underlying steel substrates due to galvanic cell formation in which Ni plays the role of cathode.

There are several ways to improve the corrosion resistance of zinc-coated steel, varying from chromating the zinc surface²⁻⁴ to its coating with organic molecules⁵ and to incorporation of useful nanoparticles in the zinc coating.^{6,7}

Zinc-nanoparticles composite coatings are meant to provide better corrosion resistance to steel than pure zinc due to the fact that the nanoparticles confer to the composite layers improved corrosion and wear resistance, increased hardness, better adhesion of future paint layers, and prolonged lifetime.⁸ Various nanoparticles such as TiO₂,⁹⁻¹² SiO₂,^{13,14} Al₂O₃,^{15,16} CeO₂,¹⁷ mixed oxides^{18,19} and carbon fibers,²⁰ and other were used for enhancing the corrosion resistance of zinc coatings.

Recently, graphene materials have attracted considerable attention due to their valuable characteristics such as high electrical and thermal conductivity, excellent mechanical properties and large surface area.^{21,22} Graphene oxide incorporated

* Corresponding author: limur@chem.ubbcluj.ro

in polymers,²³ deposited on metallic surfaces,²⁴ dispersed in the corrosive media²⁵ or used to reinforce metallic coatings²⁶⁻²⁸ represents an attractive alternative to improve corrosion resistance of metals.

Zn-graphene composite coatings on steel were prepared by electrodeposition²⁹ and reported as significantly better corrosion resistant than pure zinc. Incorporation of graphene materials into the zinc matrix hindered the formation of pits on the surface and favored the formation of hillock structures. However, no correlation between the graphene material origin or preparation method and the corrosion properties of the resulting coatings was reported.

In this context, this work investigates the effect of graphene oxide with different oxidation degree and of some experimental conditions on the corrosion behavior of Zn-graphene composite coatings. More specifically, the coatings were electrodeposited on carbon steel from an acidic electrolytic bath using four types of graphene oxides produced by graphite sono-chemical exfoliation³⁰ and a commercially available reduced graphene oxide, respectively, and the electrochemical behavior of the coatings were

corroborated with the characteristics of graphene materials.

RESULTS AND DISCUSSION

Morpho-structural investigations

Figure 1 shows the SEM images of Zn/steel (A), Zn-rGO/steel (B) and Zn-GO/steel (C) deposits.

The surface morphology is different in the three cases. The pure Zn coating contains vertical platelets, while the Zn-rGO/steel deposit contains irregular nodules distributed on the whole electrode surface. On the contrary, Zn-GO/steel deposits are more uniform and fine grained, suggesting a higher rate of deposition associated with a better interaction of GO with the Zn matrix.

These results are confirmed by EDS analysis (Table 1). It can be observed that the highest C content was recorded in the case of Zn-GO/steel deposits, which is expected, suggesting that the incorporation degree of GO is higher during the simultaneous electroreduction of Zn²⁺ ions and GO suspension than in the case of already reduced graphene (rGO).

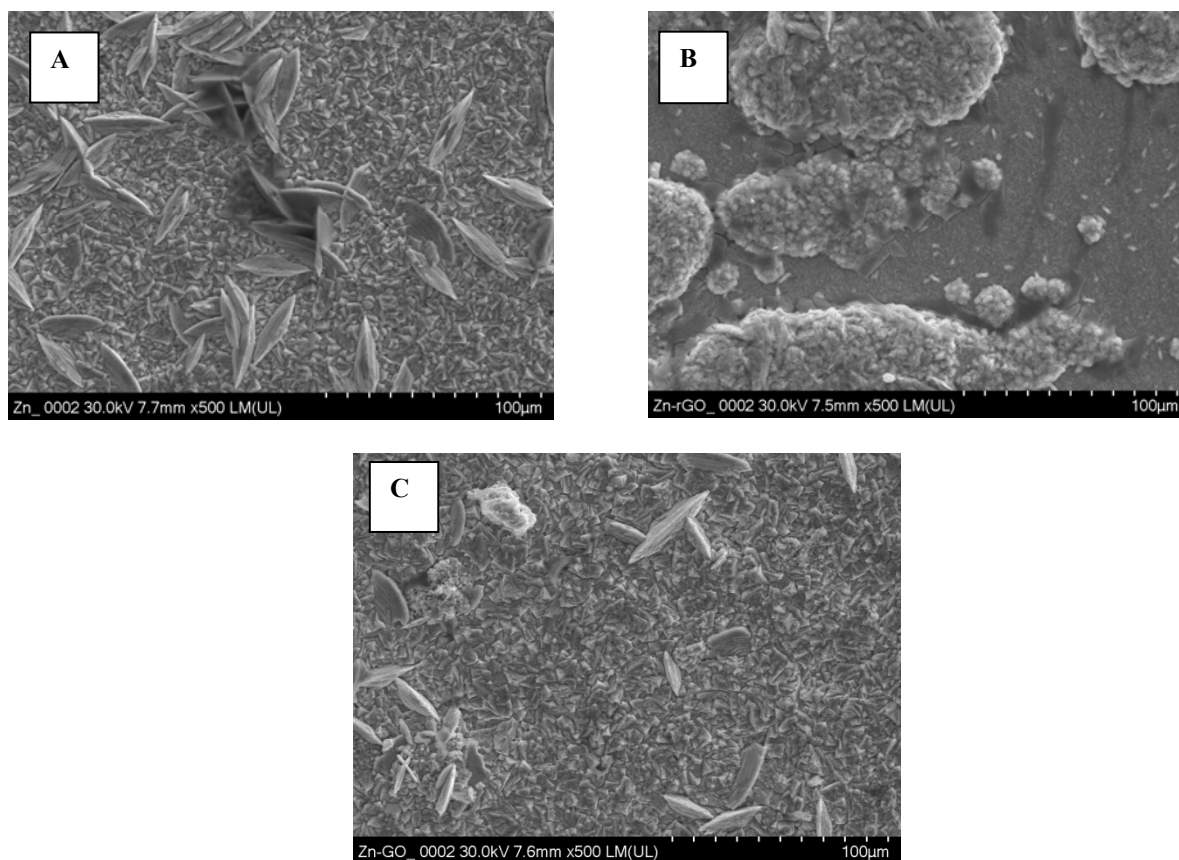


Fig. 1 – SEM micrographs of Zn/steel (A), Zn-rGO/steel (B) and Zn-GO/steel (C).

Table 1
Deposits composition determined by EDS measurements

Sample	Element content (weight %)		
	Zn/steel	Zn-GO/steel	Zn-rGO/steel
C	6	19	4
O	3	6	22
S	-	-	4
Cl	-	-	2
Na	-	-	9
Fe	-	-	11
Zn	91	75	48
Total	100	100	100

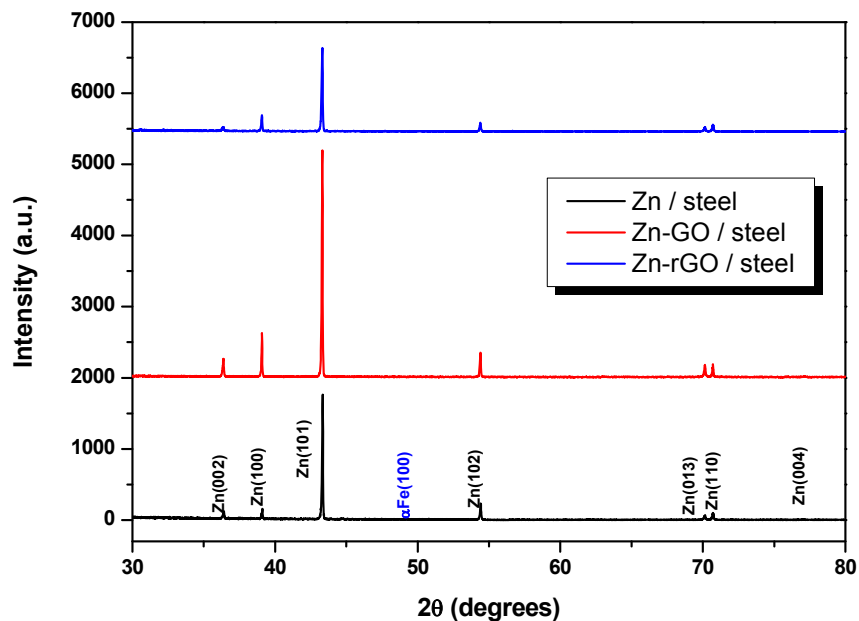


Fig. 2 – XRD spectra of Zn/steel, Zn-GO/steel and Zn-rGO/steel.

The XRD spectra of the three deposits are depicted in Figure 2. It can be observed that the texture of the deposits is not the same in all cases and that the presence of incorporated graphene material changed the microstructure of the coating. Thus, the electrochemically reduced GO incorporated in the deposit enhances the crystal growth along (101) and (100) low index crystallographic planes. These results are in agreement with those reported in the literature.²⁹

Polarization curves

Tafel polarization curves of Zn, Zn-rGO and Zn-GO coatings were recorded in the potential range of ± 250 mV against the open circuit potential of the respective coating which was used as working electrode and are presented in Figure 3.

For the composite coatings obtained with the three different GO fractions SF, OF and PF prepared by centrifugation of the initial GO suspension, the potentiodynamic curves are

presented in Figure 4. For all the coatings, the results extracted by the interpretation of the polarization curves by Tafel method are presented in Table 2.

The corrosion current density for the Zn-rGO and Zn-GO coated samples is generally lower than that of their Zn coated counterparts. This could be associated to an increase of corrosion resistance of the composite coatings as a consequence of the inclusion of GO in the metallic deposit. A possible explanation could be the change and refining of the zinc deposit microstructure in the presence of graphene materials, as observed also by other authors²⁹ and put in evidence by the before-presented morpho-structural results. The better behavior of the deposits prepared by electrochemical reduction of GO in comparison with those prepared with rGO could be due to the more uniform distribution of the graphene material resulted by simultaneous reduction of GO and Zn^{2+} ions inside the zinc matrix than in the case when commercial rGO was used. The better solubility of GO in the plating electrolyte plays also a positive

role. It should be mentioned that the presence of reduced GO influences both the anodic and cathodic branches of the polarization curves, suggesting that on one side, the coating acts as a

barrier that impedes the diffusion of dissolved oxygen towards the metallic surface and, on the other side, hinders Zn dissolution.

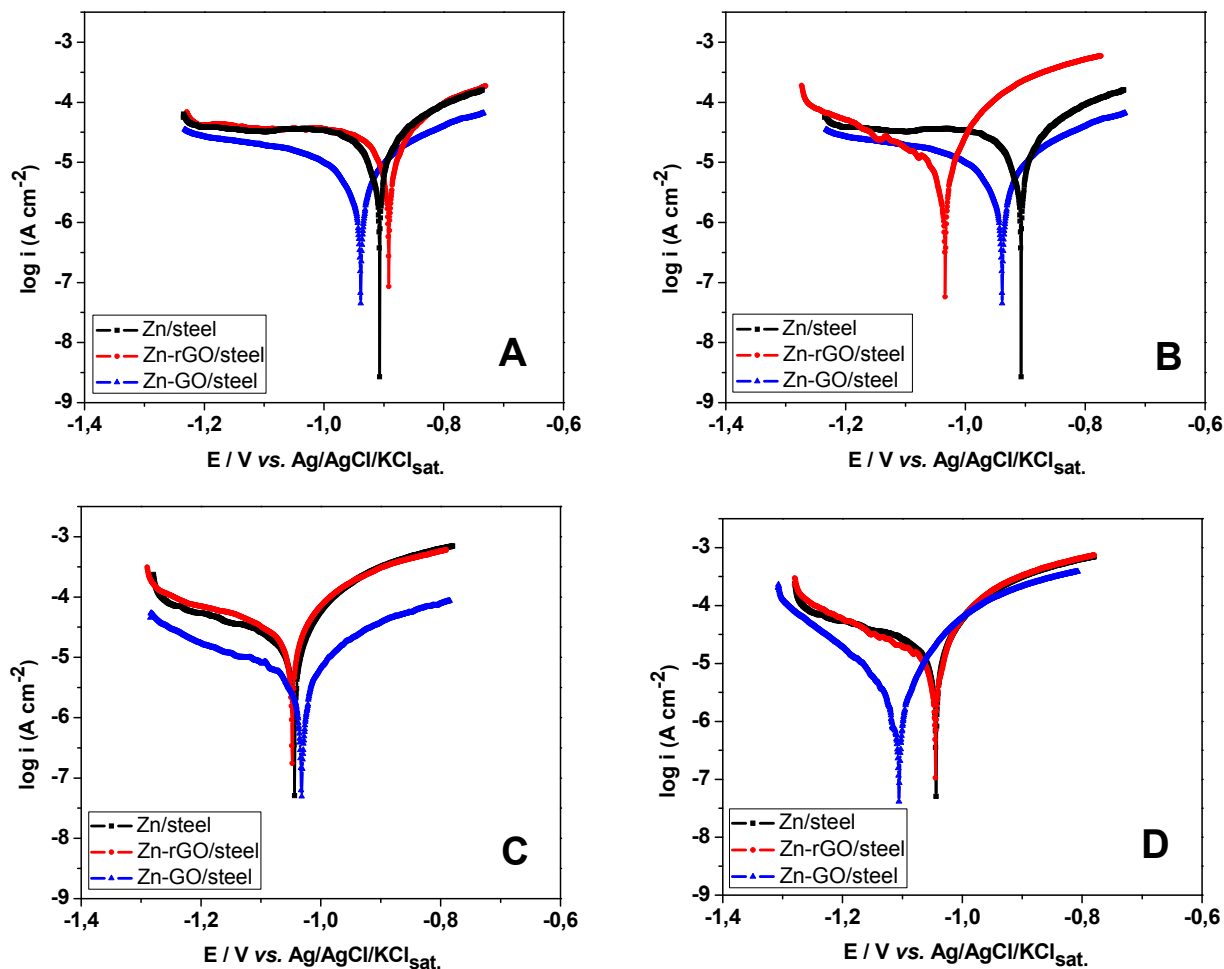


Fig. 3 – Tafel polarization curves recorded for steel coated with Zn, Zn-rGO and Zn-GO composite coatings at 20 mA/cm² with 50 mg/L graphene materials (A), and 100 mg/L graphene materials (B) and at 40 mA/cm² with 50 mg/L graphene materials (C), and 100 mg/L graphene materials (D); deposition time, 20 minutes.

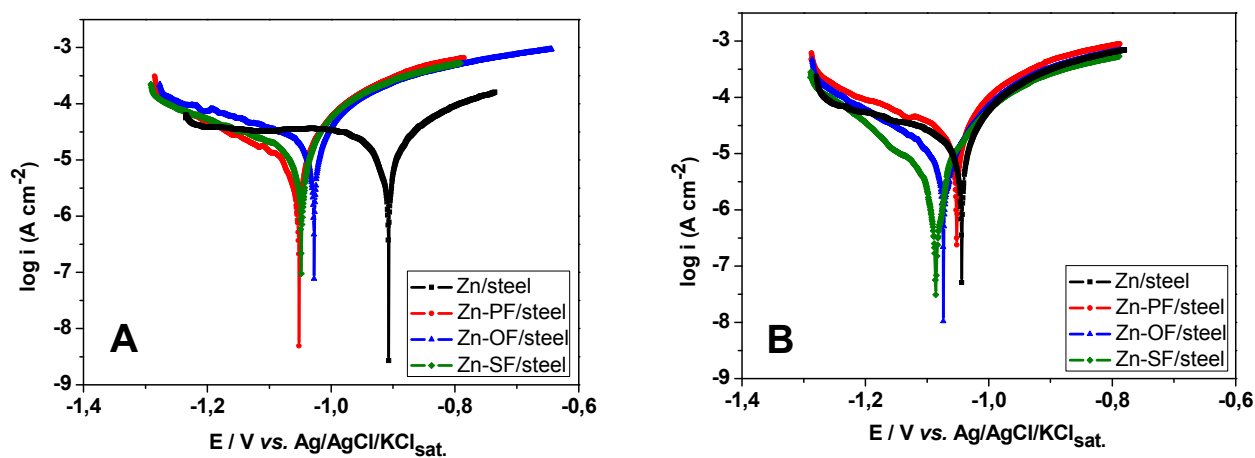


Fig. 4 – Tafel polarization curves recorded for steel covered with Zn-PF, Zn-OF and Zn-SF composite coatings at 20 mA/cm² (A) and at 40 mA/cm² (B) with 50 mg/L graphene materials; deposition time, 20 min.

Table 2

The electrochemical parameters, estimated by extrapolation of the Tafel curves for different zinc-based protective coatings on steel

Sample	Graphene concn. (mg/L)	E_{corr} (mV vs. Ag/AgCl/KCl _{sat})		i_{corr} ($\mu\text{A}/\text{cm}^2$)	
		Deposition current density (mA/cm^2)			
		20	40	20	40
Zn/steel	0	-906	-1042	21.88	21.38
Zn-rGO/steel	50	-891	-1049	18.62	23.98
Zn-GO/steel		-937	-1030	7.58	6.03
Zn-rGO/steel	100	-1034	-1044	12.02	11.09
Zn-GO/steel		-941	-1106	7.24	2.63
Zn-PF/steel	50	-1053	-1052	16.98	17.21
Zn-OF/steel		-1032	-1076	21.03	13.18
Zn-SF/steel		-1050	-1088	19.05	6.62

It can be seen that in most cases, the beneficial effect of GO fractions is more evident when 100 mg/L are used. This is in agreement with the observation that, in the case of composite coatings obtained electrolytically, the concentration of nanoparticles in the electrolyte controls their incorporation degree and is an important experimental parameter.^{9,7} The increase of electrodeposition current density from 20 mA/cm² to 40 mA/cm² does not change significantly the corrosion current density values recorded at the composite samples.

Irrespective to the current density used, a very similar behavior of the deposits containing the three different fractions PF, OF and SF is observed from Figure 4 suggesting same incorporation mechanism of these fractions in the zinc deposit. In the same time, it should be mentioned that their effect on the corrosion behavior of samples is not as important as that of electrochemically reduced GO during zinc deposition. This could be due to the lower incorporation degree of the fractions in the composite deposits, affecting their microstructure and consequently, their corrosion resistance. A dependence of the incorporation fraction on the nanoparticles characteristics was already reported for other metallic composites such as Ni-TiO₂,^{7,31} Zn-TiO₂⁹ etc. These characteristics certainly play an essential role in their incorporation mechanism and consequently, may influence the corrosion behavior of the resulting coatings.

The small differences between the corrosion current density values noticed for the three GO fractions could be explained based on some

particularities of these fractions, such as the unreacted free functional groups (associated with the oxidation degree). It was previously shown³⁰ that the ratio of the peak intensities of carbon to oxygen (C/O ratios) in XPS spectra of the graphene fractions were 1.43 for SF, 2.12 for OF and 2.20 for PF suggesting a lower oxidation degree of PF and OF, as compared with the SF fraction. This could lead to a lower incorporation degree of PF and OF fractions during electrodeposition, which contributes to the slightly lower corrosion resistance of the resulting deposits. Thus, it is confirmed once again that the preparation method and the reduction of GO is a key topic, and different reduction processes result in different properties that in turn affect the final performance of materials or devices containing rGO.³²

Electrochemical impedance spectroscopy

In order to get a deeper insight into the corrosion behavior of the newly prepared coatings, electrochemical impedance measurements were carried out at the open circuit potential immersed in a 0.2 g/L Na₂SO₄ + 0.2 g/L NaHCO₃ corrosive solution adjusted to pH = 5 with H₂SO₄. In Figure 5 are presented the Nyquist diagrams for the most resistant coating (Zn-GO/steel) and for the Zn/steel coating, as a reference after 36 hours of immersion in the corrosive solution.

To simulate the electrode/solution interface, a 2RQ parallel circuit equivalent circuit previously proposed by Kumar *et al.*²⁹ was used (Figure 6). The equivalent circuit is based on the existence of

a dielectric coating (Q_{coat}) reinforced by ionic conduction through its pores (R_{coat}). The parameter R_e is correlated with the solution resistance, while the R_{ct} - Q_{dl} parameters correspond to the charge transfer resistance at the interface coupled with the double layer pseudo-capacitance. The elements, C_{coat} and C_{dl} , represented in the circuit as capacitors, were fitted as constant phase elements (CPEs) described by the terms Q and n . The impedance of the CPE is given by the following equation:³³

$$Q = Z_{\text{CPE}(\omega)} = [C(j\omega)^n]^{-1}$$

where j is an imaginary number and ω is the angular frequency in rad/s. The values of n are associated with the non-uniform distribution of current as a result of roughness and surface defects.

It is worth mentioning that by using graphene oxide nanoparticles in the plating baths different kinetic parameters were obtained as compared to pure Zn coatings (Table 3).

The time evolution of the impedance diagrams recorded for Zn-GO/steel deposits, showed an increase of the impedance modulus in the first 36 h, reaching a relatively good and constant corrosion resistance value of the composite layer (results not shown). Moreover, after 36 h the R_p value for the composite layer overcomes the value noticed for the pure Zn layer (Figure 5). A further constant increase of R_p in the case of Zn-GO/steel coatings is noticed (Table 3), reflecting a progressive hindering of the corrosion reaction. C_{dl} is significantly decreased for the composite layer,

suggesting also a diminished activity of the surface towards corrosion.

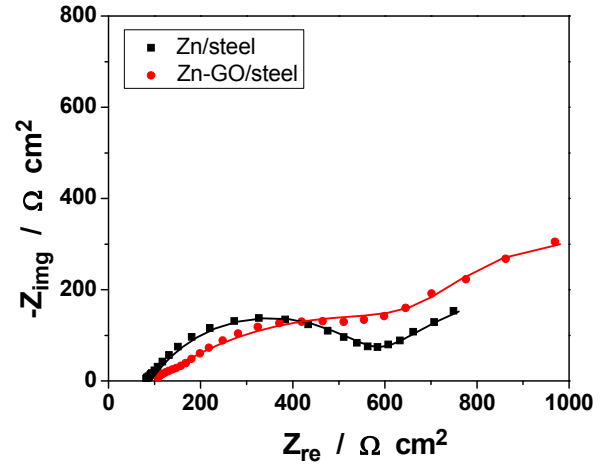


Fig. 5 – Electrochemical Impedance Spectroscopy (EIS) diagrams of steel coated with Zn and for Zn-GO/steel after 36 h immersed in 0.2 g/L Na_2SO_4 + 0.2 g/L NaHCO_3 (pH = 5). Lines represent the calculated data. Electrodeposition parameters: $i = 40 \text{ mA/cm}^2$; GO concentration in the electrolyte, 100 mg/L; deposition time, 20 minutes.

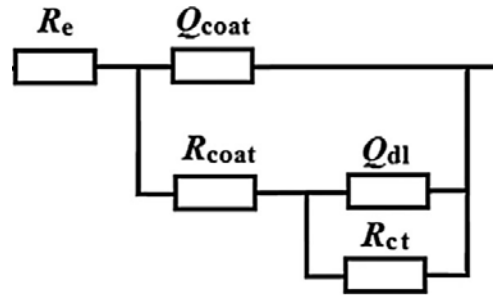


Fig. 6 – Equivalent circuit used for interpreting the experimental impedance data.

Table 3

Values of fitted parameters of the equivalent circuit for time evolution of the impedance for steel coated with Zn and Zn-GO immersed in 0.2 g/L Na_2SO_4 + 0.2 g/L NaHCO_3 (pH = 5) after 1h of immersion. Electrodeposition parameters: $i = 40 \text{ mA/cm}^2$; GO concentration in the electrolyte, 100 mg/L; deposition time, 20 minutes

Time evolution (h)	R_e ($\Omega \text{ cm}^2$)	R_{coat} ($\Omega \text{ cm}^2$)	Q_{coat} ($\text{m}\Omega^{-1} \text{ s}^n \text{ cm}^{-2}$)	n_1	C_{coat} (mF cm^{-2})	R_{ct} ($\Omega \text{ cm}^2$)	Q_{dl} ($\Omega^{-1} \text{ s}^n \text{ cm}^{-2}$)	n_2	C_{dl} (F cm^{-2})	$*R_p$ ($\Omega \text{ cm}^2$)
Zn/steel										
1	90	235	0.16	0.608	0.018	326	0.040	0.608	0.207	561
36	92	502	0.18	0.632	0.043	742	0.018	0.592	0.103	1244
48	89	610	0.16	0.647	0.043	813	0.011	0.579	0.049	1423
60	85	589	0.15	0.651	0.042	722	0.010	0.588	0.043	1311
Zn-GO/steel										
1	105	158	0.91	0.437	0.074	414	0.048	0.706	0.160	572
36	112	812	0.77	0.407	0.384	659	0.018	0.898	0.023	1471
48	104	808	0.74	0.414	0.363	685	0.017	0.914	0.022	1493
60	103	796	0.75	0.411	0.364	734	0.015	0.872	0.021	1530

EXPERIMENTAL

Materials/Synthesis

The various graphene oxides used for the electrodeposition of zinc composite coatings and their preparation modes are presented in Table 4.

The preparation and characterization of IF, SF, OF and PF was presented elsewhere.³⁰ Briefly, a mixture of H₂SO₄ (270 mL, 95-97%, Reactivul București), H₃PO₄ (30 mL, 85%, Merck), graphite (2.7 g, purum powder < 0.1 mm, Fluka) and KMnO₄ (12 g, Merck, 99%) was realized and held for 2 h in ice bath and 4 days at room temperature. After that, H₂O₂ (200 mL, 3%, Riedel-de Haën) was added to the previously obtained mixture placed in ice bath for 1 h and subsequently the suspension was centrifuged (5000 rpm, 15 min) – dispersed -sonicated (15 min) in H₂O (200 mL; one time), HCl (100 mL, 37%, Sigma-Aldrich; two times) and ethanol (100 mL, 37%, Reactivul București; two times). The obtained wet solid was dispersed in a 50% aqueous ethanol solution and sonicated again for 15 min. After 7 days, 90% of upper part of the GO suspension was harvested as initial fraction (IF) from which three distinct GO fractions – supernatant (SF), oil-like (OF) and paste-like (PF) (see Table 4) – were obtained by centrifugation (6000 rpm, 2 h).

Electrodeposition of zinc-graphene composite coatings

The electrodeposition experiments were performed in a classical cell (volume of 100 mL) with a three electrode arrangement: a steel disc impressed in a Teflon cylindrical holder was used as the working electrode ($A = 0.5024 \text{ cm}^2$), a Pt wire was used as the counter electrode and a commercial ALS RE-1B Ag/AgCl/KCl_{sat} was used as the reference electrode. The reference electrode was separated from the electrolyte bulk *via* a Luggin capillary filled with the investigated electrolyte. To prepare the working electrode for investigation, the disc shaped steel surface was polished on emery paper by different granulation (from 600 to 3000) and finally on felt with Al₂O₃ (alumina) to clean the metallic dust.

Before electrodeposition, the working electrode was ultrasonicated for 2 minutes in ethanol, then thoroughly rinsed with ethanol and distilled water in order to remove any remaining impurities from the surface.

The composition of electrolyte used in the electrodeposition process is presented in Table 5. The plating time used for electrodeposition was 20 minutes and two current densities were employed: 20 mA/cm² or 40 mA/cm². Electrodeposition process was carried out at room temperature and the plating solution was stirred at 200 rpm speed throughout the deposition process.

Table 4

Graphene oxide (GO) types used in the zinc composites electrodeposition process


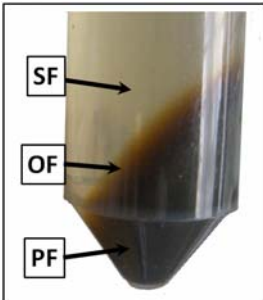

Graphene type	Origin/preparation method	Aspect
Initial water-ethanol GO suspension (IF)	Protected sono-oxidative exfoliation of graphite ³⁰	
Supernatant fraction (SF) (transparent light-brown, about 9% wt.)	Centrifugation of IF ³⁰	
Oil-like GO fraction (OF) (about 11% wt)		
Paste-like fraction (PF) (about 74% wt)		
Commercial reduced graphene oxide (rGO)	Graphenea, Spain	

Table 5

Electrolyte composition used in the electrodeposition of composite zinc-graphene coatings

Electrolyte	Composition	pH
Synthetic electrolyte ²⁹	320.4 g/L ZnSO ₄ ·7 H ₂ O 30 g/L Na ₂ SO ₄ 10 g/L NaCl 0.05 g/L CTAB	5.6

ZnSO₄·7H₂O, NaHCO₃, Na₂SO₄, NaCl and CTAB (cetyltrimethylammonium bromide) were obtained from Merck, Germany. The obtained Zn-graphene composites, in which IF of GO and commercial rGO were used, were termed as Zn-GO and Zn-rGO, respectively. Zn-PF, Zn-OF and Zn-SF were termed the composites obtained by using the three GO fractions resulted by IF centrifugation (see Table 4). The concentrations of graphene materials in the electrolytes during electrodeposition were 50 and 100 mg/L, respectively.

Corrosion tests

The corrosion tests were carried out in simulated acid rain (0.2 g/L Na₂SO₄ + 0.2 g/L NaHCO₃) adjusted with H₂SO₄ 1N to pH = 5. Open circuit potential (E_{oc}) measurements were performed as a function of time. Anodic and cathodic polarization curves were recorded in a potential range of E = E_{corr} ± 250 mV, with a scan rate of 0.166 mV/s. All electrochemical tests were performed at room temperature with computer-controlled potentiostat/galvanostat PARSTAT (Princeton Applied Research) Model 2273, compatible with PowerSuite software. Electrochemical impedance spectroscopy (EIS) measurements were carried out at E_{oc}, in the frequency range of 100 kHz-10 mHz at 10 points per decade with an AC voltage amplitude of ± 10 mV. Electrochemical impedance data were fitted using ZSimpWin 3.21 software.

Morpho-structural investigations

X-Ray Diffraction measurements (XRD) were carried out at room temperature on a Bruker D8 Advance powder diffractometer using Cu Kα₁ radiation (λ = 0.154056 nm). The θ-2θ Bragg-Brentano configuration geometry and incident-beam Ge (111) monochromator were used to investigate the structural properties of the samples. The measurements were performed in the 10–80° range in steps of 0.01°.

The Scanning Electron Microscopy (SEM) was performed using an Ultra High Resolution (UHR) SEM Hitachi 8230 system operated in high vacuum conditions. The instrument capabilities allow particular scanning options in order to show the distribution of components in relation to their chemical composition and topography of the studied surface. High resolution SEM images acquired at low landing voltage can be assessed without destruction of the samples. The SEM accelerating voltage was 15kV in a vacuum of 10⁻⁵ mbar and secondary electrons images combined with Energy Dispersion Spectroscopy (EDS) analysis were used to investigate the morphological properties.

CONCLUSIONS

Graphene material incorporation in zinc deposits can be successfully done by simultaneous

reduction of GO and Zn²⁺ ions during electrodeposition.

Electrochemical measurements (polarization measurements and electrochemical impedance spectroscopy) carried out in a 0.2 g/L Na₂SO₄ + 0.2 g/L NaHCO₃ corrosive solution adjusted to pH = 5 with H₂SO₄ demonstrated that the incorporation of graphene material in zinc enhanced the corrosion resistance of the resulting composite coatings when compared to pure zinc coating. The inhibition efficiencies determined from the values of current densities by Tafel method are higher than those determined by EIS, probably due to the longer duration of the later experiments.

Even if no spectacular differences were observed between the deposits prepared with different GO types, it can be concluded that the degree of inhibition depends on graphene incorporation degree, which depends on the GO type and its preparation mode. Understanding the electrodeposition mechanism, as well as corroborating the results of the corrosion tests with the preparation methods of GOs, could lead to better corrosion resistance performances of galvanized steel.

Future research should mainly focus on a much deeper understanding of the reduction mechanism of GO in order to obtain a non-defective graphene material, able to improve significantly the mechanical and anti-corrosive properties of composite coatings.

Acknowledgements. This work was supported from funds of TeMATIC-Art, Cod proiect: P_40_374, No. 34375/09.08.2017^o, Project co-financed by FEDR through Competitiveness Operational Programme 2014 – 2020. Funding contract: 14/01.09.2016, MySMIS: 105765. The authors would like to thank Dr. Lucian Barbu-Tudoran for SEM measurements obtained through the infrastructure from the Research Center and Advanced Technologies for Alternative Energies-CETATEA.

REFERENCES

1. B. M. Praveen, T. V. Venkatesha, Y. Arthoba Naik, K. Prashantha, *Surf. Coat. Tech.* **2007**, *201*, 5836-5842.
2. C. Gabrielli, M. Keddam, F. Minouflet-Laurent, K. Ogle, H. Perrot, *Electrochim. Acta* **2003**, *48*, 1483-1490.

3. S. F. L. Mertens, E. Temmerman, *Corros. Sci.* **2001**, *43*, 301-316.
4. E. Frackowiak, J. M. Skowronski, *J. Power Sources* **1998**, *73*, 175-181.
5. J. I. Martins, T. C. Reis, M. Bazzaoui, E. A. Bazzaoui, L. Martins, *Corros. Sci.* **2004**, *46*, 2361-2381.
6. A. Hovestad, L. J. J. Janssen, *J. Appl. Electrochem.* **1995**, *25*, 519-527.
7. C. T. J. Low, R. G. A. Wills, F. C. Walsh, *Surf. Coat. Tech.* **2006**, *201*, 371-383.
8. A. Bund, D. Thiemig, *J. Appl. Electrochem.* **2007**, *37*, 345-351.
9. A. Vlasa, S. Varvara, A. Pop, C. Bulea, L. M. Muresan, *J. Appl. Electrochem.* **2010**, *40*, 1519-1527.
10. A. Gomes, M. I. Da Silva Pereira, M. H. Mendonça, F. M. Costa, *J. Solid State Electrochem.* **2005**, *9*, 190-196.
11. T. Deguchi, K. Imai, H. Matsui, M. Iwasaki, H. Tada, S. Ito, *J. Mater. Sci.* **2001**, *36*, 4723-4729.
12. B. M. Praveen, T. V. Venkatesha, *Appl. Surf. Sci.* **2008**, *254*, 2418-2424.
13. K. Kondo, A. Ohgishi, Z. Tanaka, *J. Electrochem. Soc.* **2000**, *147*, 2611-2613.
14. T. J. Tuaweri, G. D. Wilcox, *Surf. Coat. Tech.* **2006**, *200*, 5921-5930.
15. D. Mukherjee, N. Palaniswamy, S. Guruviah, E. Belthowska, P. Barbara, *B. Electrochem.* **1990**, *6*, 380-381.
16. S. Oue, H. Nakano, S. Kobayashi, T. Akiyama, H. Fukushima, K. Okumura, *J. Surf. Finish Soc. Japan* **2002**, *53*, 920-925.
17. P. I. Nemes, M. Lekka, L. Fedrizzi, L. M. Muresan, *Surf. Coat. Tech.* **2014**, *252*, 102-107.
18. P. I. Nemes, M. Zaharescu, L. M. Muresan, *J. Solid State Electrochem.* **2013**, *17*, 511-518.
19. P. I. Nemes, N. Cotolan, L. M. Muresan, *Studia UBB Chemia, LVIII* **2013**, *1*, 81-91.
20. W. Chengfu, Y. Meifang, T. Jie, *Compos. Struct.* **1987**, *4*, 98-104.
21. H. Wang, X. Yuan, G. Zeng, Y. Wu, Y. Liua, Q. Jiang S. Gu, *Adv. Colloid Interface* **2015**, *221*, 41-59.
22. Y. Shao, J. Wang, H. Wu, J. Liu, I. A. Aksay, Y. Lin, *Electroanalysis* **2010**, *22*, 1027-1036.
23. C. Qiu, D. Liu, K. Jin, L. Fang, G. Xie, J. Robertson, *Mater. Chem. Phys.* **2017**, *198*, 90-98.
24. A. M. A. Al-Sammarraie, M. H. Raheema, *Int. J. Corros.* **2017**, 1-8. <https://doi.org/10.1155/2017/6939354>
25. A. U. Chaudhry, V. Mittal, B. Mishra, *Mater. Chem. Phys.* **2015**, *163*, 130-137.
26. C. Liu, F. Su, J. Liang, *Appl. Surf. Sci.* **2015**, *351*, 889-896.
27. Y. Raghupathy, A. Kamboj, M. Y. Rekha, N. P. Narasimha Rao, C. Srivastava, *Thin Solid Films* **2017**, *636*, 107-115.
28. Z. Ren, N. Meng, K. Shehzad, Y. Xu, S. Qu, B. Yu, J. K. Luo, *Nanotechnology* **2015**, *26*, 1-8.
29. M. K. Punith Kumar, M. P. Singh, C. Srivastava, *RSC Adv.* **2015**, *5*, 25603-25608.
30. L. C. Cotet, K. Magyari, M. Todea, M. C. Dulescu, V. Danciu, L. Baia, *J. Mater. Chem. A* **2017**, *5*, 2132-2142.
31. J. Li, Y. Sun, X. Sun, J. Qiao, *Surf. Coat. Tech.* **2005**, *192*, 331-335.
32. S. Pei, H.-M. Cheng, *CARBON* **2012**, *50*, 3210-3228.
33. Q. Ni, D. W. Kirk, S. J. Thorpe, "Electrochemical Engineering for the 21st Century", ECS Transactions, USA 2010 p. 55-72.

